Full Length Research Paper

Dielectric relaxation, electrical conductivity and impedance response of Barium titanate (BT) and Strontium titanate (ST) doped Ba(Fe$_{0.5}$Nb$_{0.5}$)O$_3$ ceramics

N. K. Singh[1]*, Pritam Kumar[1], A. Kumar[1] and S. Sharma[2]

[1]Department of Physics, Veer Kunwar Singh (V. K. S) University, Arrah, Bhojpur, 802 301 Bihar, India.
[2]Department of Physics, A. N. College, Patna, Bihar, India.

Lead-free polycrystalline ceramics of Ba(Fe$_{0.5}$Nb$_{0.5}$)O$_3$ and its solid solutions 0.91Ba(Fe$_{0.5}$Nb$_{0.5}$)O$_3$-0.09BaTiO$_3$ (BFN-BT) and 0.91Ba(Fe$_{0.5}$Nb$_{0.5}$)O$_3$-0.09SrTiO$_3$ (BFN-ST) were fabricated by a solid-state reaction process, and their electrical properties were characterized in a broad frequency range (100 Hz to 1 MHz) at a temperature range from 30 to 385°C. The prepared ceramics are single phased with monoclinic structure as confirmed by X-ray diffraction. The microstructure analysis was done by scanning electron microscope. Dielectric response show low temperature dielectric dispersion at low frequency showing space charge phenomena arising due to defects. Existence of sharp transition around (T$_c$~255°C) and broad transitions around (T$_c$~205°C) of dielectric constant (ε′) versus temperature is demonstrated in the complex perovskite in BFN-BT and BFN-ST ceramics respectively at different frequencies (10.82, 20.2 and 32.2 kHz). The relaxor property was analyzed by the broadening of the maximum dielectric permittivity as well as its shifting to high temperatures with the variation of frequency measurements. In the pure BFN ceramic, dielectric studies confirmed that the compound do not have dielectric anomaly at different frequencies (10.82, 20.2 and 32.2 kHz) and temperature ranges (30 to 385°C). The frequency-dependent electrical data are also analyzed in the framework of conductivity and impedance formalisms.

Key words: Perovskite oxides, dielectric constant, electrical properties, scanning electron micrographs.

INTRODUCTION

The dielectric properties of material are intrinsic properties expressed by the relative complex permittivity $\varepsilon^* = \varepsilon' - j\varepsilon''$, where ε' is the dielectric constant and represents the ability of a material to store electrical energy and ε'', is the loss factor and represents the loss of electric energy in the material. Amount of loss is described by a parameter loss tangent (tanδ). The dielectric parameters are generally dependent on frequency, temperature, density and other factors such as material structure and composition (Bansal et al., 2001; Nelson, 1992, 1993). The electrical properties are often represented in terms of some complex parameters like complex impedance (Z*), complex dielectric modulus (M*), and loss tangent (tanδ). They are related to each other as follows: $Z^* = Z' - j Z'' = R_s - \dfrac{j}{\omega C_s}$, $M^* = M' + j M'' = j\omega\varepsilon_0 Z^*$ and loss tangent, $\tan\delta = \dfrac{M''}{M'} = -\dfrac{Z'}{Z''}$; where j = is

*Corresponding author. E-mail: singh_nk_phy27@yahoo.com. Tel: +919431850564.

the imaginary factor, R_s and C_s are the resistance and capacitance in series (s), ω (=2πf) is the angular frequency and ε_0 is the permittivity in free space (8.854 × 10^{-12} F/m). The above three expressions offer a wide scope for graphical representation. Complex impedance spectroscopy (CIS) technique will be used to study the impedance properties/parameters of the compounds using a computer controlled LCR meter/impedance analyzer at an ac signal over a wide range of frequency and temperature. Impedance analysis basically involves the display of the impedance data in different formalism and provides us the maximum possible information about the materials. The display of impedance data in the complex plane plot appears in the form of a succession of semicircles attributed to relaxation phenomena with different time constants due to the contribution of grain (bulk), grain boundary and interface/polarization in a polycrystalline material. Hence, the contributions to the overall electrical property by various components in the material are separated out easily.

Complex perovskite oxides with high dielectric constants play an important role in various technological applications such as wireless communication systems, microelectronics and global positioning systems. High dielectric constant allows one to fabricate smaller capacitive components, thus offering the opportunity to decrease the size of the electronic devices (Agrawal et al., 2009). Various relaxation processes seem to coexist in complex perovskite ceramics, which contain a number of different energy barriers due to point defects appearing during their fabrication. Therefore, the departure of the response from an ideal Debye model in ceramic samples, resulting from the interaction between dipoles, cannot be disregarded (Bharti et al., 2009).

Simple perovskite compounds have the chemical formula ABO_3. In the cubic phase, the oxygen atoms form a cubic lattice of corner-sharing octahedra with the B cations at their centers, while the A cations form a second interpenetrating cubic sublattice located at the 12-fold coordinated sites between octahedra. Interestingly, most of the perovskite compounds that are of greatest technological interests are not simple systems, but rather complex oxides with two different kinds of B atoms of the form $A(B'B'')O_3$. Ferroelectric perovskites have been the subject of extensive studies due to their promising electrical characteristic which has a potential usefulness in fundamental research and technological applications. Investigation of the electrical properties of these materials is desirable to predict their suitability for electronic applications.

Being a lead free perovskite material, $Ba(Fe_{0.5}Nb_{0.5})O_3$ is an environmental friendly material, thus making it a good substitute for Pb containing compounds for various applications. Both A and B–sites dopants have been used to modify the electrical and dielectric properties of $Ba(Fe_{0.5}Nb_{0.5})O_3$. Not much work has been reported on B- site doping and there is hardly any extensive report on

the strontium titanate and barium titanate doping in barium iron niobate. In this article, we report dielectric relaxation, electrical conductivity and impedance response of BT and ST doped $Ba(Fe_{0.5}Nb_{0.5})O_3$ ceramics.

EXPERIMENTAL PROCEDURE

Sample preparation

In analogy to our previous work (Singh et al., 2011a, b; Singh and Kumar, 2011a) the conventional solid state reaction technique is used for the synthesis of BFN, BFN-BT and BFN-ST ceramics. The starting materials are reagent grade $BaCO_3$, $SrCO_3$, Fe_2O_3, Nb_2O_5 (M/S-Loba Chemie Pvt. Ltd.) and TiO_2 (M/S-S.D. fine), taken in stoichiometric ratio. The materials are mixed in acetone medium for 6 h and the mixture is calcined at 1200°C for 8 h and brought to room temperature by cooling at the rate of 100°C /h. The calcined sample is palletized into a disk using polyvinyl alcohol (PVA) as binder. Finally, the disk is sintered at 1250°C for 6 h and cooled down to room temperature at the cooling rate of 1°C /min.

Electrical measurement

For electrical measurement, the sintered disk (of thickness of the range of 1.28 to 1.56 mm and diameter of the range of 11.79 to 12.23 mm) is polished, electroded with fine silver paint (Alfa Aesar). Impedance parameters (Z), phase angle (θ), capacitance (Cp) and loss tangent (tanδ) were measured as a function of frequency (100 Hz to 1 MHz) at different temperatures (30 to 385°C), using a PSM (Comm.1735) in conjunction with a laboratory-made sample holder and heating arrangement with an AC signal (1.2 V).

RESULTS AND DISCUSSION

Structural and microstructural analysis

The X-ray diffraction pattern of BFN (inset), BFN-BT and BFN-ST measured at room temperature is shown in Figure 1. The pattern is characteristic of a perovskite structure. All the reflection peaks of the X-ray profile are indexed and lattice parameters are determined using a least-squares method with the help of a standard computer programme (POWDMULT) (Wul and PowdMult, 1999). Good agreement between the observed and calculated d-values (Table 1) suggests that the BFN, BFN-BT and BFN-ST ceramics crystallize in monoclinic phase at room temperature. The cell parameters with cell volume are shown in Table 2. X-ray diffraction confirms that the specimen is single phase.

The scanning electron micrograph of the samples was recorded by FEI Quanta 200 equipment to check proper compactness of all the samples is shown in Figure 2. The nature of the micrographs exhibits the polycrystalline texture of the material having highly distinctive and compact rectangular/cubical grain distributions. The grain size of the pellet sample was found to be in the range of 2 to 3 μm.
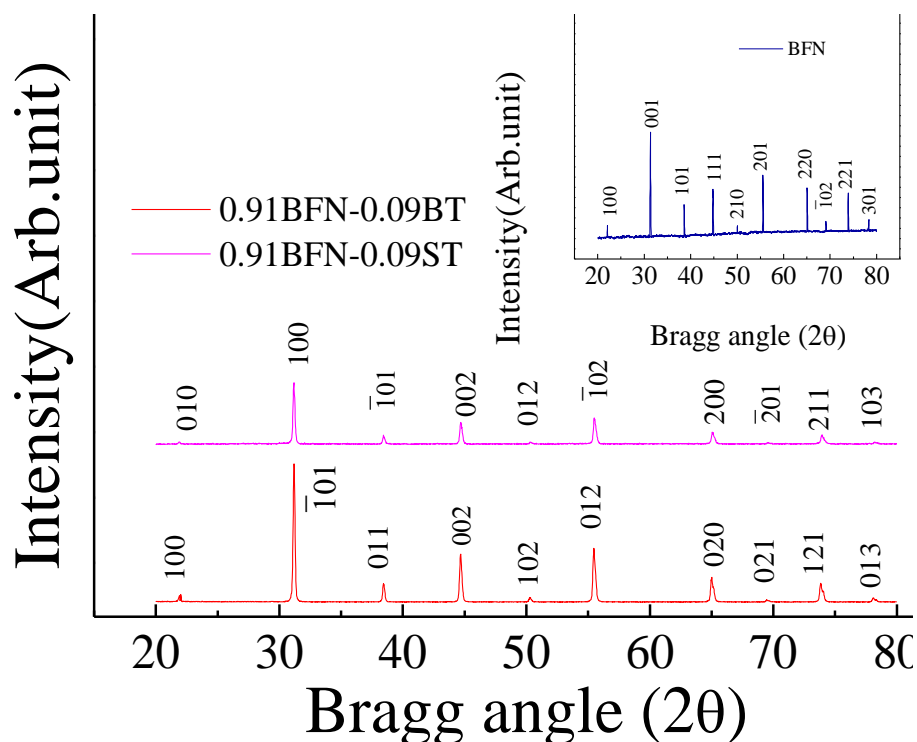
Figure 1. XRD patterns of BFN, 0.91BFN-0.09BT and 0.91BFN-0.09ST ceramics at room temperature.

Dielectric studies

The variation of relative dielectric constant (ε') and tangent loss (tanδ) of BFN, BFN-BT and BFN-ST ceramics with frequency at different temperature is shown in Figures 3 and 4 respectively. For all the samples initially, both ε' and tanδ decreases with increase in frequency, which is a general feature of polar dielectric materials irrespective of composition of the specimens. The fall in ε' arises from the fact that polarization does not occur instantaneously with the application of the electric field, which is further due to the inertia of the dipoles and the delay in response towards the impressed alternating electric field leads to dielectric loss and decline in ε'. At low frequencies, all types of polarization contributes and as the frequency is increased, polarizations with large relaxation times cease to respond and hence the decrease in ε' (Chopra et al., 2004). At lower frequencies ε' is maximum because the contributions from the space charge polarization is large. At higher frequencies, contributions from the polarizations having high relaxation time cease resulting in the decrease in ε' (Kittel, 1995). The same type of frequency-dependent dielectric behavior is found in many other perovskite ceramic systems (Singh et al., 2010a, b, 2008; Kumar et al., 2011a, b; Singh and Kumar 2011b). In BFN-BT and

BFN-ST ceramics, the tanδ peaks were observed which shift towards the higher frequency region (with rise in temperature). This type of feature suggests the presence of dielectric relaxation in the compound (Shantha and Varma, 1997; Saha and Sinha, 2006). The range of variation of ε in BFN-BT is higher than in BFN-ST and BFN ceramics, the range of ε' is 153 to 7370 for BFN-BT, 207 to 1013 for BFN-ST and 150 to 1999 for BFN ceramics at 30 to120°C.

BaTiO$_3$ (BT) with a perovskite structure is a strong dielectric material, which has far reaching applications in the electronics industry for transducers, actuators and high-k dielectrics, and is mostly used to make multilayer ceramic capacitor (MLCC) materials (Mao et al., 2003; Cui et al., 2006; Pengfei et al., 2007). On the other hand, dielectric properties of SrTiO$_3$ (ST) based materials have been widely studied (Muller and Burkhard, 1979; Bianchi et al., 1995; Ang and Yu, 1992). Fe doped SrTiO$_3$ (ST) materials, combining the required stability and interesting transport properties at relatively high temperatures, have been considered for application as electrochemical electrodes and possibly also for resistive oxygen sensors. For these applications, special attention has been paid to the electrical transport properties at high temperatures. However, work on both the dielectric and conductive properties, especially at low frequencies and low

Table 1. Comparison of some observed (obs) and calculated (cal) d-values (in Å) of some reflections of $Ba(Fe_{0.5}Nb_{0.5})O_3$, $0.91Ba(Fe_{0.5}Nb_{0.5})O_3$-$0.09BaTiO_3$, and $0.91Ba(Fe_{0.5}Nb_{0.5})O_3$-$0.09SrTiO_3$ compounds at room temperature with intensity ratio I/I_0. The estimated error in d is ± 0.0001 Å.

(hkl)	BFN d (Å)	(hkl)	$0.91Ba(Fe_{0.5}Nb_{0.5})O_3$-$0.09BaTiO_3$ d (Å)	(hkl)	$0.91Ba(Fe_{0.5}Nb_{0.5})O_3$-$0.09SrTiO_3$ d (Å)
(100)	[o] 4.0337 (17) [c] 4.0337	(100)	[o] 4.0350 (20) [c] 4.0350	(010)	[o] 4.0623 (5) [c] 4.0623
(001)	[o] 2.8553 (100) [c] 2.8553	($\bar{1}$01)	[o] 2.8643 (100) [c] 2.8643	(100)	[o] 2.8643 (100) [c] 2.8643
(101)	[o] 2.3410 (43) [c] 2.3410	(011)	[o] 2.3375 (27) [c] 2.3375	($\bar{1}$01)	[o] 2.3410 (17) [c] 2.3410
(111)	[o] 2.0213 (55) [c] 2.0213	(002)	[o] 2.0264 (45) [c] 2.0264	(002)	[o] 2.0264 (37) [c] 2.0264
(210)	[o] 1.8181 (26) [c] 1.8226	(102)	[o] 1.8124 (19) [c] 1.8090	(012)	[o] 1.8124 (4) [c] 1.8133
(201)	[o] 1.6581 (66) [c] 1.6537	(012)	[o] 1.6554 (49) [c] 1.6552	($\bar{1}$02)	[o] 1.6548 (43) [c] 1.6556
(220)	[o] 1.4331 (56) [c] 1.4331	(020)	[o] 1.4336 (31) [c] 1.4337	(200)	[o] 1.4324 (21) [c] 1.4321
($\bar{1}$02)	[o] 1.3578 (30) [c] 1.3573	(021)	[o] 1.3520 (18) [c] 1.3517	($\bar{2}$01)	[o] 1.3513 (4) [c] 1.3510
(221)	[o] 1.2816 (52) [c] 1.2800	(121)	[o] 1.2823 (28) [c] 1.2813	(211)	[o] 1.2808 (17) [c] 1.2807
(301)	[o] 1.2175(29) [c] 1.2154	(013)	[o] 1.2226 (19) [c] 1.2224	(103)	[o] 1.2211 (5) [c] 1.2211

Table 2. Structural data for $Ba(Fe_{0.5}Nb_{0.5})O_3$, $0.91Ba(Fe_{0.5}Nb_{0.5})O_3$-$0.09BaTiO_3$, and $0.91Ba(Fe_{0.5}Nb_{0.5})O_3$-$0.09SrTiO_3$ compounds.

Sample	Structure	a	b	c	β (in degree)	V
BFN	Monoclinic	4.0337 Å	4.0734 Å	2.8553 Å	90.12	46.92
$0.91Ba(Fe_{0.5}Nb_{0.5})O_3$-$0.09BaTiO_3$	Monoclinic	4.0350Å	4.0539Å	2.8674Å	90.17	46.90
$0.91Ba(Fe_{0.5}Nb_{0.5})O_3$-$0.09SrTiO_3$	Monoclinic	4.0623Å	4.0529Å	2.8643Å	90.09	47.16

temperatures, has been rarely done and needs to be accomplished.

The temperature-dependent relative dielectric constant (ε') and tangent loss (tanδ) at 10.82, 20.20 and 32.30 kHz of BFN, BFN-BT and BFN-ST ceramics is shown in Figures 5 and 6 respectively. The variation in ε' with temperature shows that it is strongly frequency and temperature dependent. In BFN ceramics, the relative dielectric constant increases linearly with rise in temperature at different frequencies (10.82, 20.2 and 32.2 kHz). However, no phase transition was observed in BFN in the experimental temperature range. A dielectric anomaly was observed in BFN-BT and BFN-ST ceramics. It is observed that peaks of the curves that is, the maximum value of dielectric constant decreases with increasing frequency. In BFN-BT and BFN-ST ceramics, the dielectric constant increases gradually with an increase in temperature up to transition temperature (Tc)
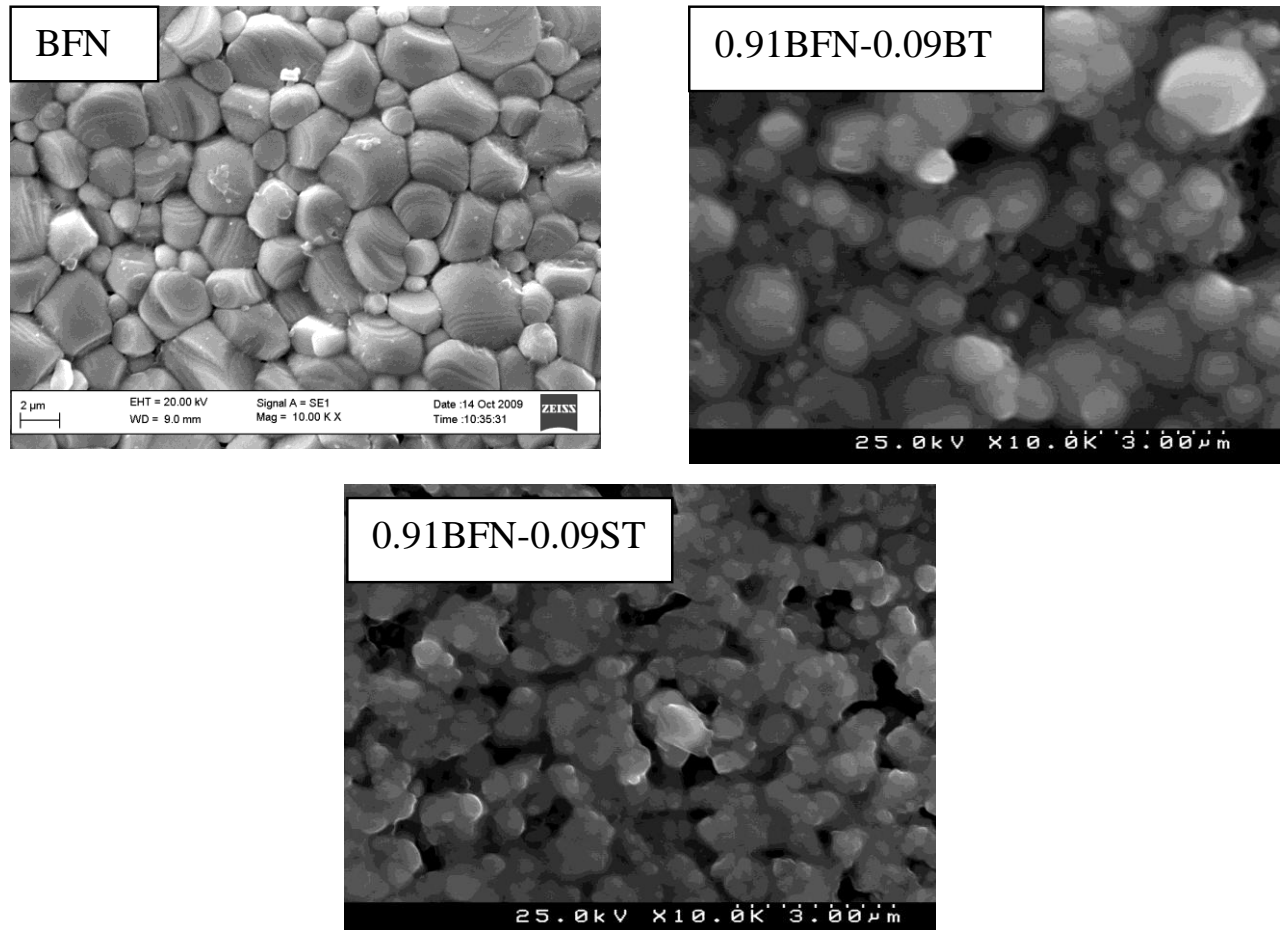
Figure 2. SEM micrographs of BFN, 0.91BFN-0.09BT and 0.91BFN-0.09ST, ceramics at room temperature.
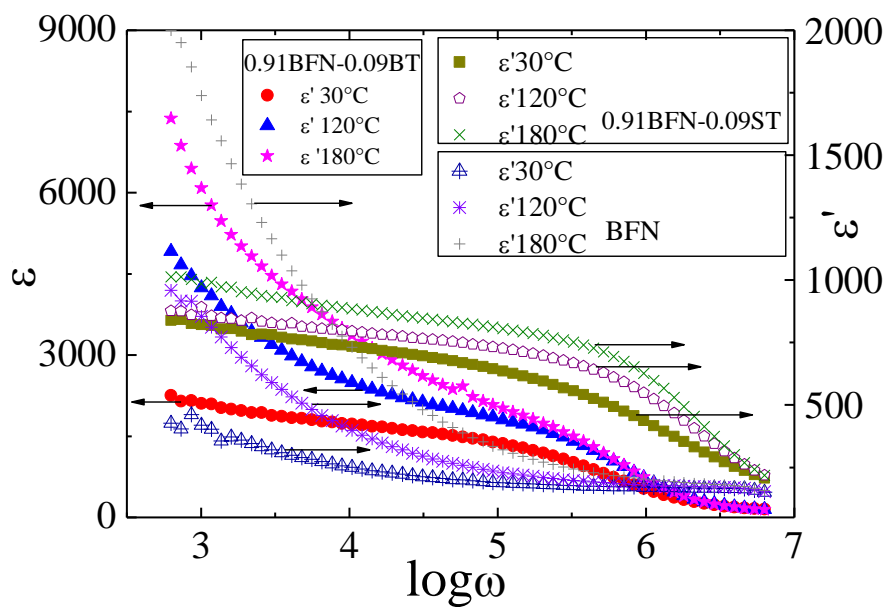
Figure 3. Logarithmic angular frequency dependence of dielectric constant (ε') of BFN, 0.91BFN-0.09BT and 0.91BFN-0.09ST, ceramics, at various temperatures.
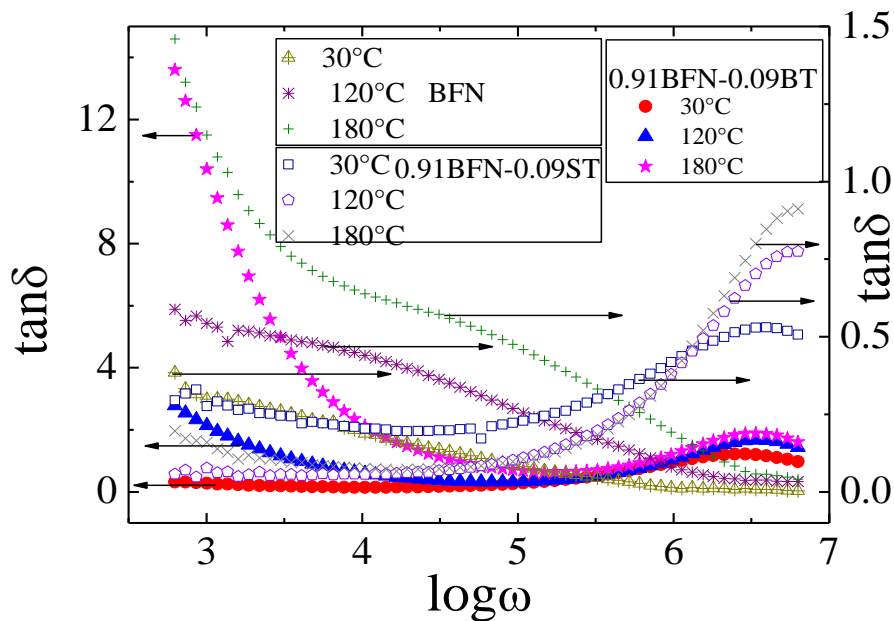
Figure 4. Tangent loss (tanδ) of BFN, 0.91BFN-0.09BT and 0.91BFN-0.09ST, as a function of logarithmic angular frequency at various temperatures.
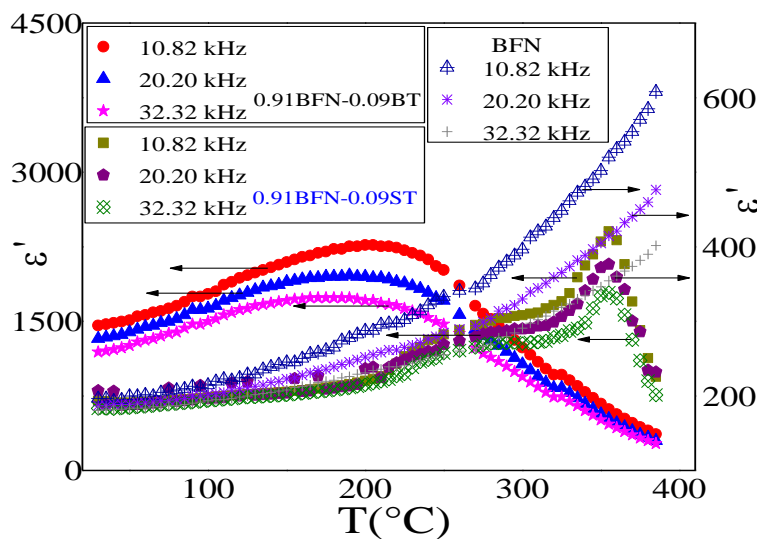
Figure 5. Dielectric constant (ε′) of BFN, 0.91BFN-0.09BT and 0.91BFN-0.09ST, ceramics as a function of temperature at selected frequencies.

and then decreases. The region around the dielectric peak is apparently broadened. The broadening or diffuseness of peak occurs mainly due to compositional fluctuation and/or substitution disordering in the arrangement of cations in one or more crystallographic sites of the BFN-BT and BFN-ST structure. It is observed from Figure 6, as the temperature increases tangent loss (tanδ) is found to increase. At low temperatures, the

molecules can not orient themselves in polar dielectrics. When the temperature rises, the orientation of dipoles is facilitated and this increases tangent loss (tanδ). At high temperatures, the dielectric losses caused by the dipole mechanism reach their maximum value and the degree of dipole orientation increases. Apart from dipole losses, electrical conduction also increases with increase temperature. These factors would cause the increase in
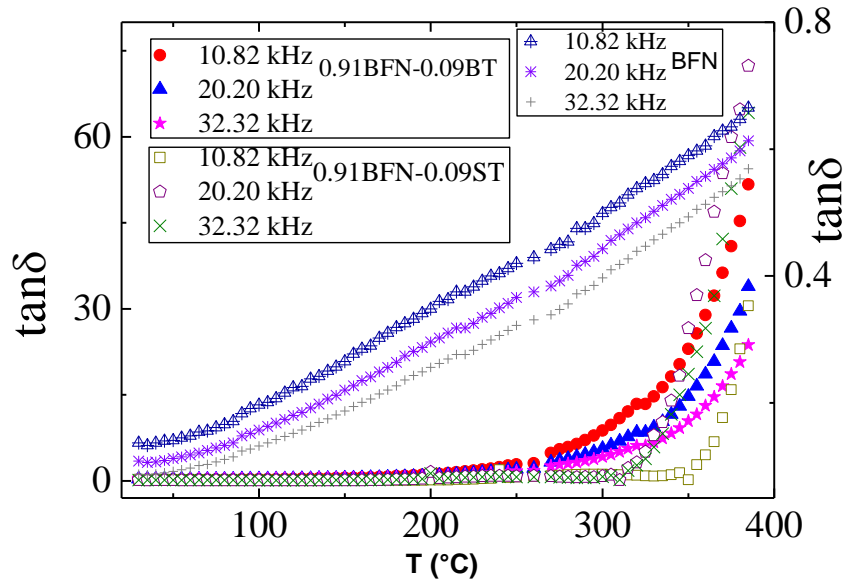
Figure 6. Tangent loss (tanδ) of BFN, 0.91BFN-0.09BT and 0.91BFN-0.09ST, ceramics as a function of temperature at selected frequencies.

tangent loss of BFN ceramics with increase in temperature (Taeev, 1975). In BFN-BT and BFN-ST, it is observed that tanδ remains almost constant up to ~305°C for BFN-ST and ~210°C for BFN-BT ceramics; afterwards, it increases rapidly.

Impedance formalism

In order to understand the dynamics of the mobile ions in BFN, BFN-BT and BFN-ST ceramics, we have plotted the angular frequency dependence of real (Z') and imaginary (Z") parts of complex electrical impedance of above ceramics in Figures 7 and 8 respectively at various temperatures. Typical curves are observed in figures. The temperature affects strongly the magnitude of resistance. At lower temperatures, Z' and Z" decreases monotonically with increase in frequency upto certain frequency and then becomes frequency independent. The higher values of Z' and Z" at low frequencies and low temperatures means the polarization is larger. The temperatures where this change occurs vary in the material with frequencies. This also means that the resistive grain boundaries become conductive at these temperatures. This also shows that the grain boundaries are not relaxing even at very high frequencies even at higher temperatures (Singh et al., 2011b).

The plot of the imaginary (Z") versus real (Z') parts of the complex impedance (Z*) (Cole–Cole plot) at temperature 180°C for BFN (inset), BFN-BT and BFN-ST ceramics is shown in Figure 9. A single arc of the impedance spectrum indicates that the electrical process in the material arises due to its bulk resistance only

(Macdonald, 1987). The intercept of the semicircular arc on x-axis is an estimate of the bulk resistance (R_b) of the material and indicates the departure from the ideal Debye behavior. Infact, this behavior exhibits the non-Debye type of relaxation phenomenon in the materials.

Conductivity formalism

It is to be noted that the high values of dielectric constant (ε') and tangent loss (tanδ) in lower frequency region do not generally correspond to bulk effect. The high values of ε' interestingly observed only at very high temperature and very low frequencies may be attributed to the fact that the free charges buildup at interfaces within the bulk of the sample (interfacial Maxwell–Wagner (MW) polarization) (Kyritsis et al., 1995) and at the interface between the sample and the electrodes space-charge polarization (Jonscher, 1983). In order to elucidate this point, the frequency dependant ac conductivity (σ_ac) at various temperatures of BFN, BFN-BT and BFN-ST ceramics is plotted in Figure 10. The real part of ac conductivity and dielectric constant (ε') and conductivity (σ) is as follows

$$\varepsilon' = \frac{C}{C_0} \tag{1}$$

$$\sigma = \omega \varepsilon_0 \varepsilon'' \tag{2}$$

Where ε_0 is the dielectric permittivity in air, C/C0 the
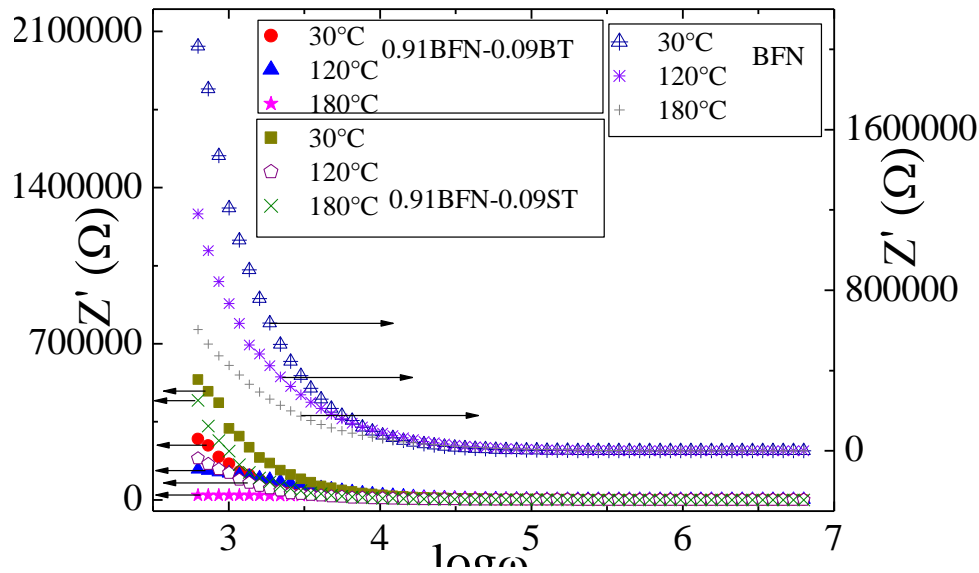
Figure 7. Z' of BFN, 0.91BFN-0.09BT and 0.91BFN-0.09ST, ceramics as a function of logarithmic angular frequency at various temperatures.
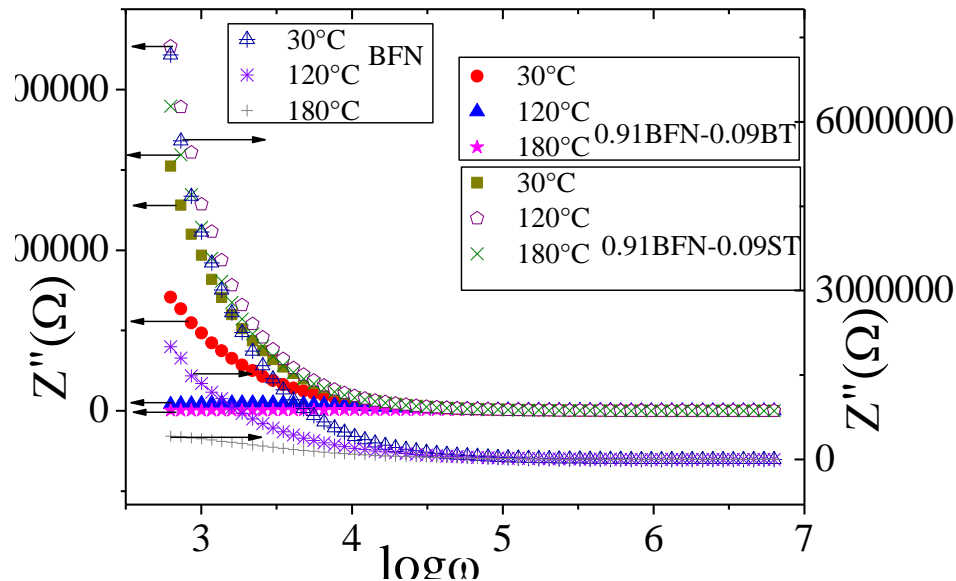
Figure 8. Z″ of BFN, 0.91BFN-0.09BT and 0.91BFN-0.09ST, ceramics as a function of logarithmic angular frequency at various temperatures.

ratio of capacitance measured with dielectric and without dielectric, ω the angular frequency and $\varepsilon'' = \tan\delta\ \varepsilon'$.

The conductivity increases with increasing frequency and increasing temperatures. For all the samples the conductivity shows dispersion which shifts to higher frequency side with the increase of temperature Notice that at low frequencies, random diffusion of charge carriers via hopping gives rise to a frequency independent conductivity. The increasing trend of $\sigma(\omega)$ in the low-frequency range may be due to the disordering cations between the neighboring sites and the presence of space charges that vanishes at higher temperatures and frequencies. The high-frequency conductivity dispersion may be attributed to ac conductivity whereas the frequency independent region of the conductivity pattern corresponds to the dc conductivity (σ_{dc}) of the
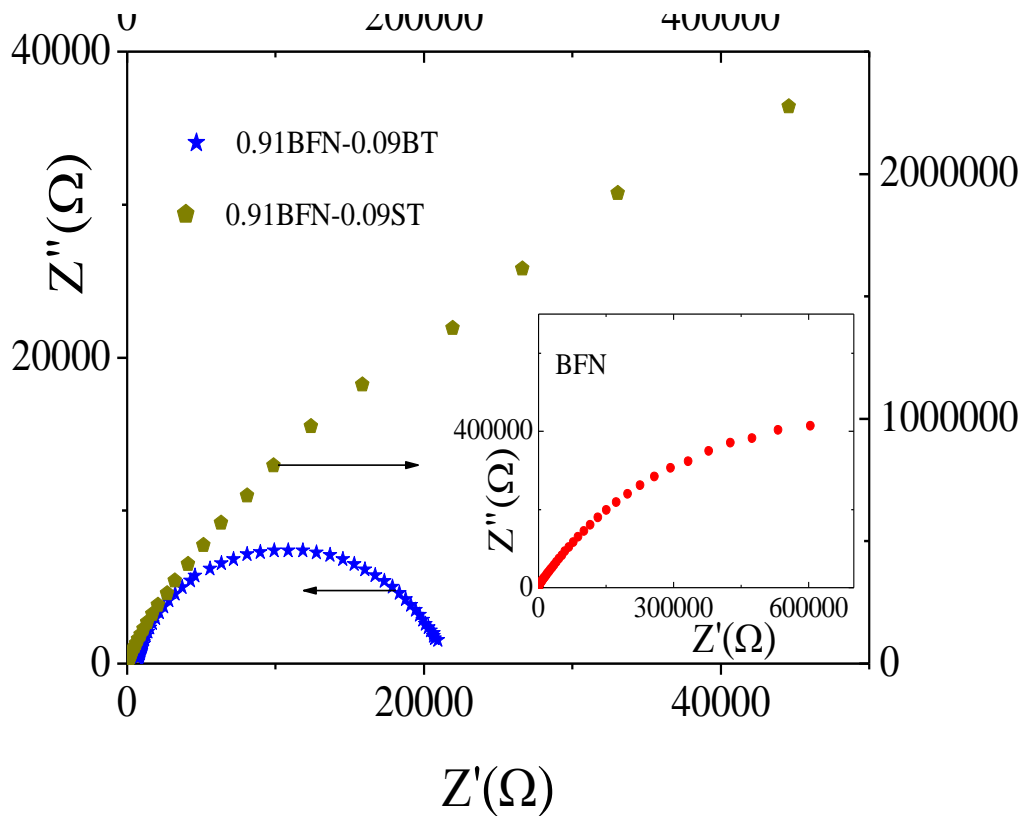
Figure 9. Complex plane impedance plot of BFN, 0.91BFN-0.09BT and 0.91BFN-0.09ST, ceramics, at 180°C.
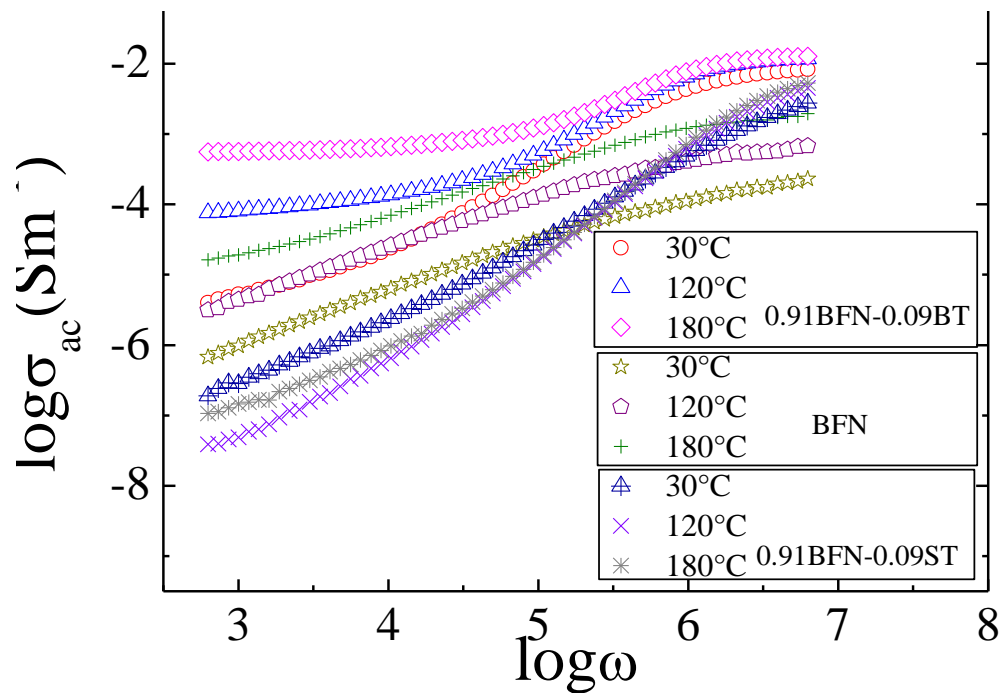
Figure 10. Logarithmic angular frequency dependence of ac conductivity (σ_{ac}) for BFN, 0.91BFN-0.09BT and 0.91BFN-0.09ST ceramics at various temperatures.

material.

Conclusion

The frequency-dependent dielectric dispersion of $Ba(Fe_{0.5}Nb_{0.5})O_3$ (BFN), $0.91Ba(Fe_{0.5}Nb_{0.5})O_3$-$0.09BaTiO_3$ (BFN-BT) and $0.91Ba(Fe_{0.5}Nb_{0.5})O_3$-$0.09SrTiO_3$ (BFN-ST) ceramics were prepared by a high temperature solid-state reaction technique and is investigated in the temperature range at 30 to 385°C and in the frequency range at 100 Hz to 1 MHz. The crystal structures of BFN, BFN-BT and BFN-ST ceramics determined by powder X-ray diffraction shows monoclinic phase at room temperature. The microstructure of the ceramics was examined by the scanning electron microscopy (SEM), and shows the polycrystalline nature of the samples with different grain sizes, which are inhomogeneously distributed through the sample surface. The variation of relative dielectric permittivity (ε') and tangent loss ($\tan\delta$) may be attributed to hopping of trapped charge carriers, which resulted in an extra dielectric response in addition to the dipole response.

ACKNOWLEDGEMENT

REFERENCES

Agrawal L, Singh BP, Sinha TP (2009). Dielectric Relaxation in Complex Perovskite Oxides $In(Ni_{1/2}Zr_{1/2})O_3$, Mater. Res. Bull. 44:1858–1862.

Ang C, Yu Z (1992). Dielectric properties and complex defect in $(Sr_{1-x}Bi_{2/3x})TiO_3$., J. Appl. Phys. 71:4451.

Bansal AK, Singh PJ, Sharma KS (2001). Microwave dielectric relaxation study of binary mixtures of cyclochexylamine with acetophenone. Indian J. Pure Appl. Phys. 39:799-803.

Bharti C, Dutta A, Shannigrahi S, Choudhary SN, Thapa RK, Sinha TP (2009). Impedance Spectroscopy, electronic structure and X-ray Photoelectron spectroscopy studies of $Pb(Fe_{1/2}Nb_{1/2})O_3$. J. Elect. Spectrosc. Relat. Phenomena 169:80–85.

Bianchi U, Dec J, Kleemann W, Bednorz JG (1995). Cluster and Domain-State Dynamics of ferroelectric $Sr_{1-x}Ca_xTiO_3$(X=0.007). Phys. Rev. B. 51:8737.

Chopra S, Sharma S, Goel TC, Mendiratta RG (2004). Effect of Annealing temperature on the Microstructure of chemically deposited Ca modified Lead Titanate Effect thin films. Appl. Sur. Sci. pp. 230-207.

Cui B, Yu PF, Tian J, Chang ZG (2006). Preparation and characterization of Co-doped $BaTiO_3$ nanosized powders and ceramics. Mater. Sci. Eng. B 133:205.

Jonscher AK (1983). Dielectric Relaxation in Solids. Chelsea Dielectric Press, London.

Kittel C (1995). Introduction to Solid State Physics. Wiley, New York.

Kumar P, Singh BP, Sinha TP, Singh NK (2011a). Ac Conductivity and Dielectric relaxation in $Ba(Sm_{1/2}Nb_{1/2})O_3$ ceramics, Physica B 406:139–143.

Kumar P, Singh BP, Sinha TP, Singh NK (2011b). X-ray and electrical properties of $Ba(Gd_{1/2}Nb_{1/2})O_3$ ceramic. Adv. Mater. Lett. 2(1):76.

Kyritsis A, Pissis P, Grammatikakis J (1995). Dielectric relaxation spectroscopy in poly(hydroxyethyl acrylates)/water hydrogels. J. Polym. Sci. Polym. Phys. 33:1737.

Macdonald JR (1987). Impedance spectroscopy emphasizing solid materials and system. New York: Wiley

Mao YB, Banerjee S, Wong SS (2003). Large Scale Synthesis of Single Crystalline Perovskite Nanostructures. J. Am. Chem. Soc. 125:15718.

Muller KA, Burkhard H (1979). $SrTiO_3$: An Intrinsic quantum paraelectric below 4K, Phys. Rev. B 19:3593.

Nelson SO (1993). Insect control studies with microwaves and other radio frequency. Bull. Entomol. Soc. Am. 19(3):157-163.

Nelson SO (1992). Measurement and application of dielectric properties of agricultural products. IEEE Trans. Instrum. Meas. 41(1):116-122.

Pengfei Y, Xue W, Bin C (2007). The Sol-gel process using organic monoacid as surfacatant. Scripta Mater. 57:623.

Saha S, Sinha TP (2006). Dielectric relaxation in $SrFe_{1/2}Nb_{1/2}O_3$. J. Phys. Chem. Sol. 67:1484–1491.

Shantha K, Varma KBR (1997). Frequency dependence of the dielectric properties of ferroelectric $Bi_2VO_{5.5}$(BiV) Ceramics. Sol. State Ion. 99:225–231.

Singh NK, Choudhary RNP, Banarji B (2008). Dielectric and Electrical Characteristics of $Nd_2(Ba_{0.5}R_{0.5})_2O_7$,(R=W, M_O). Physica B 403:1673.

Singh NK, Kumar P (2011a). Structural and Impedance Spectroscopy Study of $(1-X)BaFe_{0.5}Nb_{0.5}O_3+XBaTiO_3$. ISST J. Appl. Phys. 2(1):29-33.

Singh NK, Kumar P (2011b). Studies of Structural and Electrical behavior of Samarium Barium Tungstate ceramics. J. Adv. Dielectr. 1(4):465-470.

Singh NK, Kumar P, Kumar H, Rai R (2010a). Structural and Dielectric properties of $Dy_2(Ba_{0.5}R_{0.5})_2O_7$(R=W,Mo). Adv. Mater. Lett. 1:79-82.

Singh NK, Kumar P, Roy OP, Rai R (2010b). Structural and Dielectric properties of $Eu_2(B'_{0.5}B''_{0.5})_2O_7$(B'=Ba,B"=W,Mo). J. Alloys Compd. 507:542-546.

Singh NK, Kumar P, Rai R (2011a). Studies of Structural, Dielectric and Electrical behavior of $(1-X)BaFe_{0.5}Nb_{0.5}O_3$-XSrTiO_3. J. Alloys Compd. 509:2957–2963.

Singh NK, Pritam K, Sharma AK, Choudhary RNP (2011b). Structural and Impedance Spectroscopy Study of $BaFe_{0.5}Nb_{0.5}O_3$-$SrTiO_3$ Ceramics System. Mater. Sci. Appl. 2:1593-1600.

Taeev B (1975). "Physics of dielectric materials." Mir Publishers, Moscow.

Wul E, PowdMult (1999). PowdMult: An interactive powder diffraction data interpretation and index program, version 2.1, School of Physical Science, Flinders University of South Australia, Bedford Park, S.A. 5042, Australia.